One-dimensionally Hydrogen-bonded Silver(I) Saccharinate Complexes with *N*-(2-Aminoethyl)piperidine and *N*-(2-Hydroxyethyl)piperidine: Synthesis, Crystal Structures, FTIR and Thermal Studies

Sevim Hamamci[a], Veysel T. Yilmaz[b], and Orhan Büyükgüngör[c]

[a] Department of Chemistry, Faculty of Arts and Sciences, Ondokuz Mayis University, 55139 Kurupelit, Samsun, Turkey
[b] Department of Chemistry, Faculty of Arts and Sciences, Uludag University, 16059 Gorukle, Bursa, Turkey
[c] Department of Physics, Faculty of Arts and Sciences, Ondokuz Mayis University, 55139 Kurupelit, Samsun, Turkey

Reprint requests to Prof. Dr. V. T. Yilmaz. E-mail: vtyilmaz@uludag.edu.tr

Z. Naturforsch. **2008**, *63b,* 139 – 142; received September 5, 2007

Two new complexes [Ag(sac)(aepip)] (**1**) and [Ag(sac)(hepip)] (**2**) have been obtained by the reaction of $AgNO_3$ with $Na(sac)\cdot 2H_2O$ (sac = saccharinate) in the presence of *N*-(2-aminoethyl)piperidine (aepip) and *N*-(2-hydroxyethyl)piperidine (hepip), and characterized by elemental analysis, IR spectroscopy, thermal analysis and single crystal X-ray diffraction. Complexes **1** and **2** crystallize in the monoclinic space group $C2$ and triclinic space group $P\bar{1}$, respectively. In both complexes, silver(I) is tricoordinated. The sac ligand is N-coordinated, while aepip and hepip behave as N-N and N-O bidentate chelating ligands, respectively. The pip rings of both aepip amd hepip ligands adopt typical 'chair' conformation. The individual molecules are linked into one-dimensional chains by two N–H···O hydrogen bonds in **1**, and one O–H···O hydrogen bond in **2**. TG-DTG curves illustrated that the endothermic elimination of aepip and hepip ligands takes place in the early stages of thermal decomposition, while that of the sac moiety occurs exothermically at higher temperatures to give metallic silver.

Key words: Saccharinate Complex, Silver(I), Crystal Structure

Introduction

Saccharin ($C_7H_5NO_3S$; also named *o*-benzosulfimide) is currently the most widely used non-caloric artificial sweetener and commercially available as water-soluble alkali salts. The coordination chemistry of saccharin (Hsac) is very interesting. Metal complexes of neutral saccharin are not known, since it is readily deprotonated to its anion, saccharinate (sac). Owing to the presence of several potential sites such as the imino nitrogen, and carbonyl and sulfonyl oxygen atoms, sac may be regarded as a good polyfunctional complexing agent in coordination chemistry and forms mono-, di-, and tetrameric complexes as well as coordination polymers [1].

Our research has been focused on the preparation of new metal-sac complexes with secondary ligands. In this work, we prepared two new silver-sac complexes, with *N*-(2-aminoethyl)piperidine (aepip) and *N*-(2-hydroxyethyl)piperidine (hepip) ligands. This paper describes the synthesis, spectral, thermal, and structural characterization of [Ag(sac)(aepip)] (**1**) and [Ag(sac)(hepip)] (**2**).

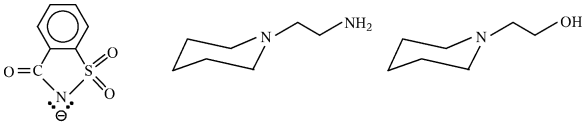

sac aepip hepip

Results and Discussion

The reaction of sodium saccharinate with $AgNO_3$ in the presence of aepip or hepip at r. t. resulted in the formation of the corresponding complexes, [Ag(sac)(aepip)] (**1**) and [Ag(sac)(hepip)] (**2**). Good quality crystals of both complexes were obtained in yields over 87 %. Complexes **1** and **2** are non-hygroscopic colorless solids, and they are soluble in acetonitrile-water mixtures and also in warm methanol and ethanol.

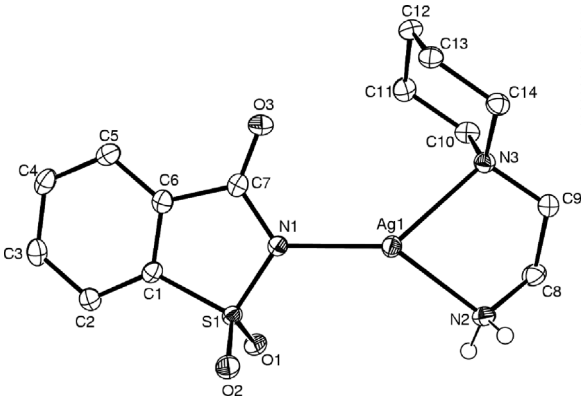

Fig. 1. A view of the asymmetric unit of **1** (displacement ellipsoids at the 40 % probability level, H atoms with arbitrary radii).

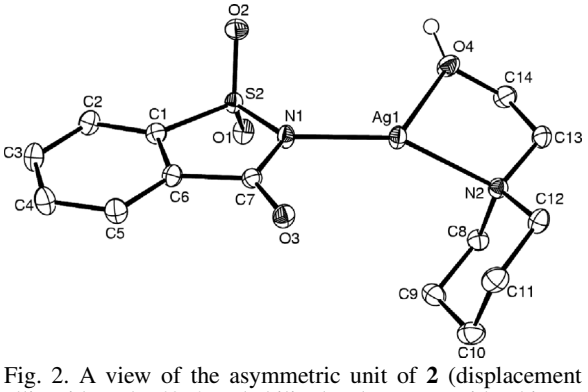

Fig. 2. A view of the asymmetric unit of **2** (displacement ellipsoids at the 40 % probability level, H atom with arbitrary radius).

Description of the crystal structures

As shown in Figs. 1 and 2, complexes **1** and **2** consist of mononuclear units. Table 1 lists their selected bond lengths and angles, together with the hydrogen bonding geometry. Complex **1** crystallizes in the monoclinic space group $C2$ with $Z = 4$, while **2** crystallizes in the triclinic space group $P\bar{1}$ with $Z = 2$. The silver(I) ion in both complexes is coordinated by a sac ligand and an aepip or a hepip ligand.

The aepip and hepip molecules act as a bidentate chelating ligands, and the Ag–N_{aepip} bond lengths are similar to those found in $[NCAg(pip)_2]_2$ [2]. The Ag–N_{sac} bonds are slightly shorter than the Ag–N_{aepip} bonds and comparable to those of the reported silver(I)-sac complexes [3 – 10], but significantly shorter than the corresponding distances of 2.449(2) Å found in $[Ag_2(sac)_2(\mu\text{-aepy})_2]$ [11]. The N–Ag–N bond angles in both complexes suggest that the silver atoms are in a distorted trigonal planar environment.

Table 1. Selected bond lengths (Å) and angles (deg), and hydrogen bonding geometry of **1** and **2**[a].

	1	**2**		**1**	**2**
Ag1–N1	2.162(2)	2.153(2)	N1–Ag1–N2	142.54(6)	153.47(6)
Ag1–N2	2.263(2)	2.269(2)	N1–Ag1–N3	137.51(6)	–
Ag1–N3	2.442(2)	–	N2–Ag1–N3	77.06(6)	–
Ag1–O4	–	2.5030(1)	N1–Ag1–O4	–	120.13(5)
			N2–Ag1–O4	–	73.71(5)

Hydrogen bonds

	D–H···A	D–H	H···A	D···A	D–H···A
1	N2–H2a···O^{i}	0.90	2.24	3.132(2)	169
	N2–H2b···O2^{ii}	0.90	2.18	3.044(2)	161
2	O4–H4a···O3^{iii}	0.93	1.99	2.714(2)	133
	C5–H5···O3^{iv}	0.93	2.59	3.263(3)	129
	C12–H12a···O2^{v}	0.97	2.53	3.192(3)	125

[a] Symmetry operations: [i] $1-x, 1+y, 1-z$; [ii] $1-x, y, 1-z$; [iii] $x-1, y, z$; [iv] $-x, 1-y, 1-z$; [v] $1-x, 1-y, 1-z$.

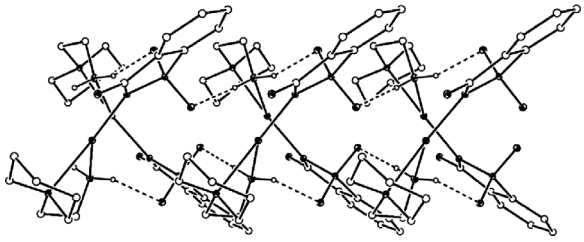

Fig. 3. A fragment of the hydrogen bonded chain of **1**.

The sac ligand is essentially planar. The puckering parameters of the pip ring are q = 0.580(3) Å and θ = 3.32(2)° in **1**, and q = 0.586(3) Å and θ = 2.30(3)° in **2**, suggesting that the pip rings exhibit an essentially "undistorted" (cyclohexane-like) chair conformation. The individual molecules are cross-linked by hydrogen bonds. In the crystal structure of **1**, two strong N–H···O hydrogen bonds between the amine hydrogen atoms of the aepip ligand and the sulfonyl O atoms of a sac ligand result in an arrangement with one-dimensional character (Fig. 3). Again, hydrogen bonds appear to play a role in establishing the molecular packing in **2**. The molecules assemble into a one-dimensional chain by strong O–H···O hydrogen bonds (Fig. 4). These chains are further connected by weak C–H···O interactions and C–H···π(sac) interactions [C–H···$C_g(1-x, 1-y, 1-z)$ = 2.96 Å] into a three-dimensional network.

IR spectra

The IR spectrum of **1** displays a number of absorption bands attributed to vibrational modes of

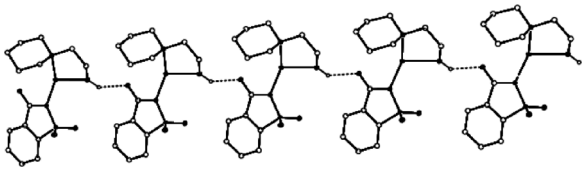

Fig. 4. A fragment of the hydrogen bonded chain of **2**.

aepip at 3350 cm^{-1} for $\nu_{as}(NH_2)$ and 3384 cm^{-1} for $\nu_s(NH_2)$, while the broad band centered at 3400 cm^{-1} is assigned to the ν(O–H) vibration of the hydroxyl group of hepip in **2**. The bands between 2800–3100 cm^{-1} are due to the aromatic or aliphatic ν(CH) stretching vibrations. The main interest in the IR spectra of the compounds **1** and **2** lies in the bands associated with the vibrational modes of the carbonyl and sulfonyl groups of the sac ligand as they can be very useful for the diagnosis of their coordination mode. The ν(C=O) mode of the sac anion appears as a sharp band centered at 1663 and 1667 cm^{-1} in the spectra of **1** and **2**, respectively, and corresponds to the coordination mode of the N-bonded sac [12]. Very strong bands at *ca.* 1270 and 1160 cm^{-1} characterize the antisymmetric and symmetric stretching frequencies of the sulfonyl group, respectively. The symmetric and antisymmetric stretching vibrations of the CNS moiety of the sac anion are observed at around 1350 and 970 cm^{-1} as sharp bands. The IR bands in the region of 650–900 cm^{-1} can be assigned to the CH in-plane and out-of-plane bending modes.

Thermal analysis

The thermal behavior of complexes **1** and **2** was studied by DTA and TG in a static atmosphere of air. Both complexes follow a similar decomposition process. Complex **1** is stable up to 146 °C and then begins to decompose with a continuous mass loss. The DTA peaks at 208 and 298 are likely to correspond to elimination of the aepip ligand. Two highly exothermic DTA processes at 491 and 537 °C characterize the decomposition of sac ligands in air [13]. The decomposition of **1** is complete at 562 °C and the total experimental mass loss value of 73.88 % agrees well with the calculated value 74.21 %, assuming that the remaining solid residue is metallic Ag.

Complex **2** decomposes at 123 °C. The first decomposition stage between 123 and 169 °C corresponds to a mass loss of 7.62 %, which is possibly due to the elimination of a C_2H_4 or CH_2O group of hepip (calcd. 7.39 %). Similar observations were in the decomposition of some divalent transition metal(II) complexes of sac with triethanolamine and 2-(2-aminoethylamino)ethanol, due to the degradation of their ethanolic groups [14]. The solid residue is stable up to 220 °C and decomposes with a continuous mass loss. Again, the DTA curve displays an exothermic peak at 276 °C, probably due to the complete degradation of the hepip ligand. Two extremely exothermic processes at 453 and 490 °C leave metallic Ag at 524 °C (total mass loss: found 73.85 %, calcd. 74.26 %).

Table 2. Crystallographic data for **1** and **2**.

	1	**2**
Empirical formula	$C_{14}H_{20}AgN_3O_3S$	$C_{14}H_{19}AgN_2O_4S$
M_r	418.27	419.24
Crystal size, mm^3	0.56×0.35×0.20	0.52×0.28×0.13
T, K	100 (2)	100 (2)
Radiation, λ, Å	0.71073	0.71073
Crystal system	monoclinic	triclinic
Space group	$C2$	$P\bar{1}$
a, Å	18.5752(14)	8.1208(14)
b, Å	5.7380(3)	9.5561(16)
c, Å	16.4508(14)	11.5472(17)
α, deg	90	103.589(13)
β, deg	116.430(6)	99.467(13)
γ, deg	90	110.255(12)
V, $Å^3$	1570.1(2)	786.9(3)
Z	4	2
D_c, $g\,cm^{-3}$	1.770	1.770
μ, mm^{-1}	1.432	1.432
$F(000)$	848	424
θ Range, deg	2.21/27.07	1.88/27.83
Index range h, k, l	±23, ±7, −20/+21	±10, ±12, ±155
Reflections collected	11112	13426
Independent reflections	3467	3715
R_{int}	0.043	0.069
Absorption correction	numerical	numerical
Min. / max. transmission	0.54 / 0.72	0.63 / 0.85
Data / parameters	3467 / 200	3715 / 199
Goodness-of-fit on F^2	1.072	0.991
Final R indices [$I \geq 2\sigma(I)$]	0.017	0.023
$wR2$ (all data)	0.040	0.053
x (Flack)	0.04(2)	–
Largest diff. peak/hole, e $Å^{-3}$	0.45/−0.39	0.76/−0.80

Experimental Section

Materials and measurements

All reagents were purchased and used without further purification. Elemental analyses (C, H and N) were carried out on an Elementar Vario EL elemental analyzer. The FT-IR spectra were recorded from KBr pellets in the range 4000–400 cm^{-1} by using a JASCO FT/IR-430 spectrophotometer. Thermal analysis curves (TG and DTA) were obtained using a Rigaku TG8110 thermal analyzer in a static air atmosphere at a heating rate of 10 °C min^{-1}.

Synthesis of the silver(I) complexes

The addition of Na(sac)·$2H_2O$ (0.24 g, 1 mmol) dissolved in 3 mL of distilled water to the solution of $AgNO_3$ (0.17 g, 1 mmol) in 5 mL of distilled water resulted in a milky suspension which was dissolved by the addition of acetonitrile (25 mL). *N*-(2-Aminoethyl)piperidine (0.13 g, 1 mmol) was added to the solution, and the mixture was allowed to stand in darkness at r. t. Colorless prismatic crystals of **1** were obtained within three days. Yield 92 %. – $C_{14}H_{20}N_3O_3SAg$ (418.27): calcd. C 40.20, H 4.82, N 10.04; found C 40.37, H 4.96, N 10.33.

The method of preparation for **2** was the same as described for **1** with *N*-(2-hydroxyethyl)piperidine instead of *N*-(2-aminoethyl)piperidine. Colorless prisms were formed by slow evaporation of the resulting solution in darkness at r. t. after two days. Yield 87 %. – $C_{14}H_{19}N_2O_4SAg$ (419.24): calcd. C 40.10, H 4.57, N 6.68; found C 40.65, H 4.42, N 6.50.

X-Ray crystallography

The data collection was performed at 100 K for both complexes on a Stoe-IPDS-2 diffractometer with graphite monochromated MoK_α radiation ($\lambda = 0.71073$ Å). The structures were solved by Direct Methods (SHELXS-97 [15]) and refined by full-matrix least-squares methods (SHELXL-97 [15]). All non-hydrogen atoms were easily found on the difference Fourier map and refined anisotropically. All hydrogen atoms were included using a riding model. The details of data collection, refinement and crystallographic data are summarized in Table 2.

Crystallographic data have been deposited with the Cambridge Crystallographic Data Centre as supplementary publication no.s CCDC 659544 (**1**) and CCDC 659545 (**2**). Copies of the data can be obtained free of charge from The Cambridge Crystallographic Data Centre *via* www.ccdc.cam.ac.uk/data_request/cif.

[1] E. J. Baran, V. T. Yilmaz, *Coord. Chem. Rev*. **2006**, *250*, 1980 – 1999.
[2] G. A. Bowmaker, C. Pettinari, B. W. Skelton, N. Somers, N. A. Vigar, A. H. White, *Z. Anorg. Allg. Chem*. **2007**, *633*, 415 – 421.
[3] R. Weber, M. Gilles, G. Bergerhoff, *Z. Kristallogr*. **1993**, *206*, 273 – 274.
[4] S. W. Ng, *Z. Kristallogr*. **1995**, *210*, 206 – 209.
[5] V. T. Yilmaz, S. Hamamci, C. Thone, *Z. Anorg. Allg. Chem*. **2004**, *630*, 1641 – 1644.
[6] S. Hamamci, V. T. Yilmaz, W. T. A. Harrison, *J. Mol. Struct*. **2004**, *734*, 191 – 195.
[7] V. T. Yilmaz, S. Hamamci, W. T. A. Harrison, C. Thone, *Polyhedron* **2005**, *24*, 693 – 699.
[8] S. Hamamci, V. T. Yilmaz, W. T. A. Harrison, C. Thone, *Solid State Sci*. **2005**, *7*, 423 – 429.
[9] S. Hamamci, V. T. Yilmaz, W. T. A. Harrison, *Struct. Chem*. **2005**, *16*, 379 – 383.
[10] V. T. Yilmaz, S. Hamamci, C. Kazak, *Z. Anorg. Allg. Chem*. **2005**, *631*, 1961 – 1965.
[11] S. Hamamci, V. T. Yilmaz, W. T. A. Harrison, *Z. Naturforsch*. **2005**, *60b*, 978 – 983.
[12] P. Naumov, G. Jovanovski, *J. Mol. Struct*. **2001**, *563/564*, 335 – 339.
[13] H. Icbudak, V. T. Yilmaz, H. Olmez, *J. Therm. Anal*. **1998**, *53*, 843 – 854.
[14] V. T. Yilmaz, Y. Topcu, A. Karadag, *Thermochim. Acta* **2002**, *383*, 129 – 135.
[15] G. M. Sheldrick, SHELXS/L-97, Programs for Crystal Structure Determination, University of Göttingen, Göttingen (Germany) **1997**.